Published in final edited form as:
Methods. 2013 April 1; 60(2): 151–160. doi:10.1016/j.ymeth.2013.03.010.

Tracking Unfolding and Refolding Reactions of Single Proteins using Atomic Force Microscopy Methods

Paul J. Bujalowski[1] and **Andres F. Oberhauser**[1,2,3]

[1]Department of Biochemistry and Molecular Biology, University of Texas Medical Branch at Galveston

[2]Department of Neuroscience and Cell Biology, University of Texas Medical Branch at Galveston

[3]Sealy Center for Structural Biology and Molecular Biophysics, University of Texas Medical Branch at Galveston

Abstract

During the last two decades single-molecule manipulation techniques such as atomic force microscopy (AFM) has risen to prominence through their unique capacity to provide fundamental information on the structure and function of biomolecules. Here we describe the use of single-molecule AFM to track protein unfolding and refolding pathways, enzymatic catalysis and the effects of osmolytes and chaperones on protein stability and folding. We will outline the principles of operation for two different AFM pulling techniques: length clamp and force-clamp discuss prominent applications. We provide protocols for the construction of polyproteins which are amenable for AFM experiments, the preparation of different coverslips, choice and calibration of AFM cantilevers. We also discuss the selection criteria for AFM recordings, the calibration of AFM cantilevers, protein sample preparations and analysis of the obtained data.

Keywords

single-molecule; biophysics; atomic force microscopy; protein folding; unfolding; osmolytes; chaperones

1. Introduction

Since its invention in 1986 (1) the AFM has evolved from being an resolution imaging tool to a versatile technique used to manipulate and detect single molecules (2-9) as well as to measure the interaction forces between single proteins (10-12). Single-molecule techniques harness several different disciplines of science (biology, physics, chemistry, material science and computer science) allowing better analysis and understanding of protein function with unprecedented resolution. Here we will discuss the study of the unfolding and refolding pathways using single molecule force spectroscopy (SMFS) techniques. This technique was developed during the 1990s and allows doing experiments at the single-molecule level under physiological relevant conditions. One of the main advantages of this technique is that it

Corresponding author: afoberha@utmb.edu.

allows tracking the structural dynamics during protein folding reactions and can capture transient folding intermediates and misfolded states that cannot be identified by bulk studies. Another advantage of single-molecule AFM is the relatively easy sample preparation. One of the most important applications of SMFS has been done in the field of protein folding/unfolding (4, 5, 7, 8, 13-32). SMFS has been also used to investigate enzyme catalysis as well as the effects of osmolytes and molecular chaperones on protein folding (33-36). In this paper we describe SMFS operating principles, practical implementation and we will discuss a few noteworthy examples.

2. Basic Principles of Single-molecule Force Spectroscopy Methods

2.1. SMFS Instrumentation

The AFM is composed of two main parts: a XYZ stage scanner (sometimes separated into Z and XY stages) and an optical head (Figure 1A). A small cantilever plays the role of microscopic force sensor, a thin and flexible piece of silicon (about 200 μm in length and 10 μm in thickness) that ends with a small pyramid-shaped stylus. A laser beam is shined on the back of the cantilever in order to track the cantilever bending when it contacts the sample (Figure 1). The force is measured using Hooke's law, $F = k_c \Delta x$, where Δx represents the cantilever deflection, k_c spring constant (stiffness of the cantilever). The optical signal bouncing off the end of the cantilever is then amplified in such a way that a small bending of the cantilever, of only a few nanometers, results in a large change in the photovoltage of the detector. The SMFS method can measure forces in range of 1 to more than 1000 piconewtons and changes in the length of proteins with nanometer and millisecond resolution (4, 27, 29, 32, 37, 38). The most common SMFS modes are the length-clamp (Figure 2A), which yields a force-extension curve and the force-clamp, which gives an extension-time curve (Figure 2C).

2.2. Length-clamp mode

By moving the sample away from the AFM tip, a stretching force is applied to the protein. The length-clamp (or constant velocity) mode records force-extension curves obtained by pulling a single protein in the *z* axis (Figure 2B). The interpretation of force-extension curves is not always straightforward. The recorded force peaks can originate from many sources which include not only the unfolding of protein domains but also detachment of other molecules from any of the two anchoring points or disentanglement of molecules. This problem was solved by using native multi-domain proteins (such as titin, tenascin or spectrin) (4, 39, 40) or recombinant polyproteins (41-44). For multi-domain and polyproteins proteins the recorded force-extension curve resembles "sawtooth" pattern which represents the sequential unfolding of individual domains. This periodicity allows unequivocal identification of single molecules. The typically forces required to unfold single proteins are in the range of 50 to 500 pN (at pulling speeds of about 1 μm/s) (2).

2.3. Force-clamp mode

The force-clamp mode controls the force applied to a protein through a feedback mechanism that maintains the applied force constant and quickly corrects the distance between the coverslip and the AFM tip. The force feedback is based on a proportional, integral, and differential (PID) amplifier whose output is connected directly to the piezoelectric positioner (45, 46). The time response of the feedback and piezo is critical. The frequency response of current PID amplifiers and piezoelectric positioners are limited to 5-10 milliseconds, which in most cases is adequate to study the unfolding and refolding reactions. However, recent advances in piezos and PID amplifiers have pushed the limit in the sub-millisecond range (about 150 μs (38)). These new high-speed force-clamp spectrometers allow the study the recoil dynamics of single polypeptide chains under force (38). The force-clamp mode allows

the precise control of the end-to-end distance of the protein with nanometer resolution (13, 45). For example, when a constant stretching force is applied to a multidomain protein (such as titin) or a polyprotein, the domains unfold stochastically in an all-or-none fashion leading to a stepwise increase of the end-to-end length of the protein (Figure 2B). Force-clamp SMFS techniques are currently being used to tackle fundamental problems in biology such as protein folding (13, 47-49) and chemical mechanisms in enzyme catalysis (25, 33, 50-55). Force-clamp SMFS techniques allow the direct measurement of the mechanical stability of proteins (energy barriers) and the kinetics of unfolding and refolding pathways and the location of kinetic barriers (13, 45, 46, 54, 56-60).

2.4. Preparation of surface-the choice of coverslips

In SMFS experiments the protein of interest is immobilized on a substrate and then by physisorption (*i.e.*, nonspecific adsorption) the protein is attached to the tip of cantilever therefore being caught between coverslip and cantilever. For immobilization purposes the protein constructs are commonly engineered with terminal cysteine-tags and then adsorbed onto a gold-coated coverslip; the interaction of gold with thiol groups is quite strong and ruptures at around 1 nN (61). If the protein of interest has solvent exposed cysteine residues then terminal histidine tags can be used for immobilization on nickel-nitriloacetic acid (Ni-NTA) functionalized coverslips (62, 63). A potential disadvantage is that the unbinding forces between His-tag and Ni-NTA are around 50 pN and thus are lower than typical unfolding forces of Ig-like domains (>100 pN) but compatible with spectrin, ankyrin or C2 domains (they unfold at forces <50pN).

2.4.1. Glass coverslips—Glass coverslips (12 or 15 mm diameter, 1 oz, Ted Pella, Inc.) should be cleaned by thoroughly spraying them with 70 % ethanol, rinse them with MilliQ water and then sonicate them for 30 minutes in 10 % (v/v) Hellmanex solution. The coverslips are then washed with water and sonicated for 30 minutes in MilliQ water. Before use coverslips should be dried using a stream of nitrogen gas.

2.4.2. Gold coated glass coverslips—Gold-coated coverslips are prepared by depositing a layer of chromium/nickel (1 nm) and then a 50 nm layer of high-purity gold (99.9%; Goodfellow), under vacuum, at a pressure of $1–2 \times 10^{-6}$ mbar using a vacuum evaporator (the chromium coating is necessary to achieve strong bonding between gold and glass)(64, 65).

2.4.3. Nickel-NTA coated glass coverslips—Glass coverslips (20-40 Round Glass Coverslips, 15 mm diameter, 1 oz, Ted Pella, Inc.) are placed in a plastic container containing 20 N KOH for 13 hour. The KOH solution is discarded; the coverslips are washed with water and transferred into a aqueous solution containing 0.02% (v/v) acetic acid and 2 % (v/v) 3-mercaptopropyltrimethoxysilane. They are placed in a 90°C oven for about 1 hour. The coverslips are washed with water and dried. The SH silane groups are reduced with 100 mM Dithiothreitol (DTT). The coverslips are rinsed with water and reacted with 20 mg/ml N-[5-(3-maleimidopropylamido)-1-carboxypentyl]iminodiaacetic acid (Dojindo Molecular Technologies, Inc.) in 10 mM 3-(N-morpholino)propanesulfonic acid-KOH (pH 7.0) for 30 minutes. The coverslips are rinsed again with water. Finally the coverslips's surface is activated by a reaction with 10 mM $NiCl_2$ for 10 minutes, rinsed with water and stored at room temperature in a glass desiccator (66).

2.5. AFM cantilevers – choice and calibration

There are two main physical parameters of AFM cantilevers that are important for SMFS experiments: the spring constant, k_c, and the resonant frequency, f_c (38, 64, 67). The spring constant affects the force sensitivity and the resonant frequency limits the response time of

the measurements. The ideal cantilevers for SMFS measurements are those with small k_c (< 10 pN/nm, for high force sensitivity) and high f_c (>1 kHz, for high response time). For example, Bruker MLCT cantilevers have a k_c and f_c of about 20 pN/nm and 1 kHz (measured in water) and Olympus Biolever BL-RC150VB cantilevers have a k_c and f_c of about 40 pN/nm and 10 kHz, respectively. The BL-RC150VB cantilevers are much smaller than the MLCT (60 μm vs 300 μm in length) and hence have a much lower viscous drag coefficient making them ideal for experiments requiring a very fast response time and low force noise (38).

The AFM cantilever spring constant can differ significantly from the value given by the manufacturer; therefore it has to be calibrated before each experiment (31). The most commonly used method for determining the spring constant of a cantilever is the thermal method, which models the cantilever as a damped simple harmonic oscillator fluctuating in response to thermal noise (11, 68, 69). The mechanical properties of the cantilever are related to the frequency and amplitude of these oscillations. Hence, its spring constant can be calculated using the so-called equipartition theorem: $<\Delta x^2> = k_b T/k$, where $<\Delta x^2>$ represents the mean-square displacement noise, k_b is the Boltzman constant and T is temperature. This calculation has a typical error of ±20% (11, 70). It must be noted also that the position of the spot on the back of the cantilever has an influence on the determination of its spring constant and that a method has been developed to correct this effect (71). An alternative method to the thermal noise one is based on the shift in the resonance frequency of the cantilever after the addition of a small mass. This method is more accurate but it requires specialized equipment (72).

2.6. Construction of Polyproteins for SMFS experiments

In order to construct polyproteins several recombinant DNA techniques and cloning methods have been developed (41-44). The polyproteins are expressed in *E. coli* strains and then purified by affinity chromatography.

2.6.1 Cloning and Expression Strategies—DNA fragments preparation: design proper primers to amplify the target protein DNA fragments and introduce different restriction enzyme sequences on both ends of each target DNA fragment using PCR. Then, the target fragments are purified, introduced into an expression vector and the proteins are then expressed using standard protocols (41-44, 73).

2.6.2 Polyprotein Purification—The *E. coli* expressing the polyproteins are dissolved in lysis buffer containing protease inhibitors and are lyzed by sonication or by using a French press. Ni-NTA resins are normally used to purify polyproteins. Before use, the resins should be equilibrated with buffer. Then, the supernatant of cell lysate is mixed with the resin. The binding process takes around 30-60 min at 4°C with gentle agitation to keep the resin completely mixed with lysate. The resin is settled by gravity and the supernatant is collected. Then, the resin is rinsed with wash buffer (containing 25 mM imidazole) several times before adding the elution buffer (containing ~250 mM imidazole). The proteins are eluted by adding the elution buffer and stored at 4°C. The proteins are then identified and analyzed by sodium dodecyl sulfate polyacrylamide gel electrophoresis (SDS-PAGE) (66).

2.7. Protein sample preparation for SMFS experiments

In a typical experiment, a small aliquot of the purified polyproteins (~1-10 μl, 10-100 μg/ml) are allowed to adsorb onto gold or Ni-NTA coated glass coverslips for about 5-10 minutes and then rinsed with buffer (usually with phosphate buffered saline (PBS)) to remove unbound proteins. The AFM tip is brought into contact with the coverslip for several seconds to allow a polyprotein to attach to the tip. Then the tip is retracted; stretching a

single polyprotein should result in a characteristic sawtooth unfolding pattern. The probability of picking up a protein is characteristically very low (about 5%) because the concentration of proteins has to be kept low enough to ensure pulling of single molecules. Additionally the contact between AFM tip and protein occurs at random locations thus most of the AFM protein traces do not show the unfolding of all the domains.

2.8. Analysis of traces

The elasticity of the unfolded polypeptide is commonly analyzed using the worm-like chain (WLC) model of polymer elasticity (4, 74, 75).

$$F(x) = \frac{k_b T}{p}\left[\frac{1}{4}\left(1 - \frac{x}{L_c}\right)^{-2} - \frac{1}{4} + \frac{x}{L_c}\right]$$

The WLC equation predicts the entropic restoring force (F) generated upon extension (x) of a protein in terms of its contour length (L_C) and persistence length (p) which characterizes the orientational correlation of segments in the chain. This analytical approximation is used to fit the WLC model to experimental force-extension curves (75, 76); to include stiffness of the chain, a modified WLC chain with “elastic modulus” parameter can be used (77). Using AFM and optical tweezers several groups have determined the persistence length of single unfolded polypeptide chains to range between 0.3 and 1.0 nm (4, 43, 75, 78-83). It is significant that this length is approximately equivalent to the distance of 0.4 nm between alpha carbon atoms in a polypeptide chain.

The AFM recordings are selected using the following criteria: i) the trace should have clean initial force-extension after retraction from the surface (i.e. little or no unspecific interactions); ii) force-extension curves of single polyproteins should have detachment forces higher than 300 pN (most domains unfold at forces in the range of 50-200 pN) to be sure that the protein is completely extended and unfolded. Typically about 1 in 500-1000 of force-extension traces fulfill these criteria. The initial contour length of the folded protein (L_c) and the contour length increments (ΔL_c) are estimated by fits of the WLC model to the force-extension curves that lead to each force peak; the zero length point is defined as the point where the AFM cantilever tip contacts the coverslip. These parameters are estimated from hundreds of force-extension recordings and used to construct unfolding force and increase in contour length histograms.

3. Tracking Protein Unfolding Reactions

When weak interactions responsible for the mechanical resistance of a protein fold are broken due to the external applied force the protein unfolds. In the force-extension traces the distance between the two consecutive peaks represents increase of the contour length which is characteristic for the each protein fold. Thus it becomes a “molecular fingerprint” because that allows the unmistakable identification of the multi-domain protein. The first studies of protein unfolding reactions using AFM were done using the sarcomeric striated muscle protein titin (4) and the extracellular matrix protein tenascin (39). These showed characteristic sawtooth patterns with regular spaced force peaks. In these unfolding SMFS experiments the recorded unfolding peaks correspond to the unfolding of single-protein domains (Figure 2A, B).

The force-clamp experiments generate length-time traces at a fixed force (Figure 2C). Each step in the length-time trace represents an unfolding event. The height represents the change in the contour length after unfolding of protein at applied force (Figure 2D). The dwell time between steps is related to the mechanical stability of the protein (84). Additionally the

force-clamp mode allows obtaining the kinetic parameters of the unfolding reaction such as unfolding probabilities, unfolding dwell-time distributions, unfolding and folding trajectories or ensemble of transition states (13, 45, 46, 57, 59, 60, 85).

SMFS has been used to track the mechanoenzymatics of giant protein kinases (86-89). The titin kinase domain is involved in strain sensing that occurs during muscle activity. The mechanical properties of the kinase domain and flanking Ig/Fn domains of the *Caenorhabditis elegans* titin-like proteins twitchin and TTN-1 were studied using SMFS (89). AFM pulling experiments showed that kinase domains have mechanical resistance and they unfold in a biphasic, stepwise fashion at forces ~50 pN and ~80 pN. The first step probably represents movement of the autoinhibitory domain from the catalytic pocket. Unfolding of the kinase domain requires application of additional force. The obtained results strongly suggest that titin kinase function as a force sensor. The conformational changes during strain-induced activation of human titin kinase domain have been also studied using SMFS (90). The process is regulated by two autoinhibition mechanisms. In the first one ATP binding site is blocked by C-terminal regulatory tail and the second one includes tyrosine autoinhibition of the catalytic base by tyrosine-170. The pulling experiments indicated that mechanical force is able to activate titin kinase due to its capacity to release the active site for ATP binding by unfolding of the autoinhibitory domain. The forces required for activation of ATP binding are lower than the forces of unfolding the surrounding titin domains.

During the last decade SMFS has been applied to investigate the mechanisms of enzyme catalysis (50-52, 91, 92). In these studies the force-dependence of an enzymatic reaction were measured by applying a mechanical force on the substrate of the reaction. An excellent example here is the investigation of reduction of disulfide bond by thioredoxins enzymes (33, 34, 53, 54). First, the polyprotein composed of I27 modules with engineered disulfide bonds between residues 32 and 75 was constructed. Then, the AFM force-clamp mode was applied to track the unfolding of domains up to disulfide bonds. In presence of thioredoxins disulfide bonds are reduced allowing the unfolding of region of the domain that previously remained inaccessible. Studies of both *E. coli* and human thioredoxins showed that the reaction rate decrease as a function of the applied force. Interestingly, different force dependence patterns were observed once applied force exceeds 200 pN. Additionally, the reduction rate accelerated with increasing force for *E. coli* thioredoxin whereas it became force-independent when human thioredoxin was present. These studies were expanded to different thioredoxins allowing the identification of two evolutionary lines of organisms: one for bacteria and the second for archaea and eukaryotes (93).

4. Tracking Protein Refolding Reactions

The SMFS has also been used to study protein refolding reactions (25, 26, 94, 95). In these experiments the protein is first stretched and then is allowed to refold by bringing back the AFM tip close to the coverslip. Folding can be observed by stretching the protein again under high force which results in protein unfolding (Figure 3).

Refolding studies have been performed using a variety of proteins such as titin, tenascin, fibronectin, filamin, calmodulin, ankyrin and ubiquitin (4, 13, 39, 96-99). For example, analysis of the refolding kinetics of the titin-like protein projectin using SMFS shows that this protein functions according to a folding-based-spring mechanism (100). Projectin is a member of the titin protein superfamily that is found in invertebrate muscles and is responsible for the high passive stiffness of insect indirect flight muscles, which are crucial to perform oscillatory work during flight. The refolding kinetics of projectin was studied using a double pulse protocol in which the time interval is changed (Figure 4A); the data

shows that projectin domains require only milliseconds to refolding (Figure 4B). Remarkably, this protein can be subjected to hundreds of stretching - relaxation cycles with no signs of rundown or fatigue indicating a unique mechanical robustness (Figure 4C). The length-clamp mode was used to investigate the refolding of projectin domains under force (Figure 5). During the experiment a single projectin was first unfolded to 70 pN and then the force was dropped to 5 pN to give it time to refold to its native state. As the figure shows before the protein reached its fully collapsed state, there was a dramatic increase in the noise level with large fluctuations length which may reflect the transient formation of secondary structures or intermediate folded states (100). Then the stretching of the protein was repeated by stepping back the force to 70 pN. The experiments clearly indicated that projectin domains can refold under relatively high forces suggesting a robust refolding mechanism that may operate over a large range of sarcomere lengths.

Force-clamp SMFS techniques have been used to investigate the refolding pathways of single ubiquitin proteins (13). In these experiments a ubiquitin polyprotein was stretched at a high force, and then force was released allowing observation of the folding process. The recorded folding trajectories were divided into distinct stages. The first stage is very fast and most likely represents the elastic recoil of the unfolded polypeptide which is caused by the change in the pulling force. The second stage is characterized by a long-lasting relaxation plateau and an increase in length fluctuations whereas the third stage is marked by an abrupt decrease in the end-to-end length, reflecting the collapse to the native folded state. The results clearly showed that folding speed of the protein depends on applied force and contour length of the unfolded protein. This study supports the notion that protein folding under force is characterized by a continuous collapse rather than by a discrete all-or-none process.

Recently, SMFS techniques were used to investigate unfolding and refolding pathways of the transmembrane protein KpOmpA (16). This protein mediates bacterial adhesion and in course of its function it is subjected to mechanical stress. SMFS experiments showed a stepwise unfolding of the protein where some of the β-strands unfolded in cooperative manner. The KpOmpA protein refolded back into the membrane after the tensile load was released. The results suggest that KpOmpA may use a stepwise unfolding mechanism to reduce the mechanical stress applied to membrane. These data suggest that cells may employ both unfolding and refolding pathways of transmembrane proteins to perform different cellular tasks.

5. Computer Simulations of Mechanical Unfolding and Folding Reactions

SMFS experiments can resolve the forces required to unfold a protein with single amino acid resolution (101, 102) but they do not provide detailed structural information. Further atomic-level description of unfolding pathways is often obtained by complementing the experimental SMFS studies with steered molecular dynamics (SMD) simulations (103-105). The magnitude of the forces observed in the SMD simulations does not directly correspond to those measured with AFM. This is partially because the pulling speeds are several orders of magnitude different. However, the simulations are qualitatively consistent with the SMFS experimental data. SMD simulations have been extensively used to examine the mechanical unfolding of a wide variety of proteins (103, 104, 106-109). The synergy between experimental data and computer simulations has significantly enhanced our understanding of protein structure and dynamics.

Recent AFM force-clamp spectroscopy experiments confirmed important computational predictions regarding the energy profiles of protein folding (85). Statistical theories of protein folding predict that proteins fold through a number of small conformational

ensembles along a rugged funnel-like energy landscape surface (110, 111). Single protein force-clamp spectroscopy experiments directly confirmed the existence of an ensemble of collapsed states that were able to convert to folded states, demonstrating the vast diversity of the collapsed conformations (85).

6. Probing Osmolytes and Molecular Chaperones using SMFS

SMFS has been used to analyze the effect of osmolytes and molecular chaperones on protein stability and folding. Osmolytes such as trehalose, sorbitol or trimethylamine *N*-oxide (TMAO) can act as "chemical chaperones" and are potent stabilizers for many proteins and capable of reversing protein misfolding and or aggregation (112-114). Several neurodegenerative diseases such as Alzheimer's, Huntington's and Parkinson's have been attributed to problems associated with protein misfolding and aggregation. There is considerable interest in developing new effective therapies based on small molecules for the treatment of these devastating pathologies. Promising results on the modulation of protein aggregation by naturally occurring osmolytes have been recently reported (112-117). Hence, the use of osmolytes as chemical chaperones to stabilize proteins/peptides that misfold and aggregate in neurodegenerative diseases is an attractive concept for drug development.

Recent studies have shown that the mechanical properties of proteins can be affected by presence of osmolytes (118-120). Increasing concentration of urea which is a well known denaturing osmolyte results in a remarkable d ecrease in the mechanical stability of PKD (polycystic kidney disease) domains (35) (Figure 6A). Addition of protective osmolytes such as sorbitol and trimethylamine N-oxide effectively counteract the effect of urea (Figure 6B). The refolding rate of PKD domains was found to decrease significantly in presence of urea but it is restored to near normal rates when sorbitol or trimethylamine N-oxide were added.

SMFS has been used to study the effects of molecular chaperones on the folding of the motor domain of myosin (36). Molecular chaperones assist in the folding of proteins (121). Myosins are actin-dependent motor proteins that convert chemical energy from ATP hydrolysis into mechanical work. They play essential roles in a wide variety of cellular motility processes, ranging from muscle contraction to cleavage furrow ingression during cytokinesis. Type II myosin heavy chains have a molecular weight of ~225 kDa and consist of an amino-terminal globular motor (or head) domain and carboxyl-terminal rod domain. The motor domain harbors the sites for actin-binding and enzymatic activity. In contrast to the rod domain, the motor domain folds in a chaperone-dependent fashion (122-126). Expression of myosin motor domains in bacteria results in misfolding. Molecular chaperones appear necessary for de novo folding and structural maintenance of the myosin head. The interaction between myosin and its chaperone UNC-45 were analyzed using SMFS techniques by coupling titin I27 domains to the myosin motor domains (127). By chemically coupling a titin I27 polyprotein to the motor domain of myosin, a "molecular reporter" was introduced providing a specific attachment point and a well characterized mechanical fingerprint in the AFM measurements. This approach enabled the study of the folding pathway of the motor domain and directly track the effects of the chaperone UNC-45. Single molecules of derivatized full length myosin (Figure 6C) or the motor domain were subjected to repeated cycles of mechanical stretching, separated by a waiting time of 10 s at zero force. The I27 unfolding pattern is apparent in the initial unfolding trace (1), but absent in the second (2) and third (3) traces, indicating that the unfolded motor domain interferes with refolding of the I27 domains. The characteristic low-force plateau stemming from the rod (between dashed lines) is visible in all traces in Figure 6C, indicating the rod folds as an independent entity and is not affected by misfolding of the motor domain. In the absence of UNC-45, the I27 saw-tooth pattern is observed only in the initial unfolding

cycle, indicating that the misfolded motor domain interferes with the refolding of the I27 domains. In the presence of 1 μM UNC-45, full recovery of folded I27 domains is observed (Figure 6D). These results indicate that the I27 domains function as a reporter for motor domain misfolding. UNC-45 seems to prevent the interference between the motor domain and the I27 units, presumably by binding to the myosin motor domain and preventing its misfolding (127). This approach should be applicable to elucidate chaperone-substrate interactions of different biological systems.

7. Perspectives

Single-molecule force spectroscopy methods are providing us with fundamental information on how proteins fold and work. This field has grown at an impressive rate during the last 20 years and SMFS methods are becoming an indispensable tool used in biophysics and biochemistry. We have gained essential information on protein-based elasticity, mechanism of protein-protein interactions, unfolding/refolding reactions, chaperone action as well as enzymatic catalysis. A key challenge of future experiments is to apply SMFS methods to study unfolding and refolding reactions of proteins in environments that more closely mimic those found in living cells. This will require the combination of SMFS with single-molecule fluorescence techniques (such as fluorescence resonance energy transfer) which should enable us to look deeper inside into the mechanism of protein folding and misfolding.

Acknowledgments

This work was funded in part by NIH grant R01DK073394, by the UTMB Claude Pepper Older Americans Independence Center NIH/NIA Grant P30 AG024832 and the John Sealy Memorial Endowment Fund for Biomedical Research.

References

1. Binnig G, Quate CF, Gerber C. Atomic force microscope. Phys Rev Lett. 1986; 56:930–933. [PubMed: 10033323]
2. Oberhauser AF, Carrion-Vazquez M. Mechanical biochemistry of proteins one molecule at a time. J Biol Chem. 2008; 283:6617–6621. [PubMed: 18195002]
3. Puchner EM, Gaub HE. Force and function: probing proteins with AFM-based force spectroscopy. Curr Opin Struct Biol. 2009; 19:605–614. [PubMed: 19822417]
4. Rief M, Gautel M, Oesterhelt F, Fernandez JM, Gaub HE. Reversible unfolding of individual titin immunoglobulin domains by AFM. Science. 1997; 276:1109–1112. [PubMed: 9148804]
5. Rief M, Oesterhelt F, Heymann B, Gaub HE. Single Molecule Force Spectroscopy on Polysaccharides by Atomic Force Microscopy. Science. 1997; 275:1295–1297. [PubMed: 9036852]
6. Ke C, Humeniuk M, H SG, Marszalek PE. Direct measurements of base stacking interactions in DNA by single-molecule atomic-force spectroscopy. Phys Rev Lett. 2007; 99:018302. [PubMed: 17678193]
7. Marszalek PE, Oberhauser AF, Pang YP, Fernandez JM. Polysaccharide elasticity governed by chair-boat transitions of the glucopyranose ring. Nature. 1998; 396:661–664. [PubMed: 9872313]
8. Marszalek PE, Lu H, Li H, Carrion-Vazquez M, Oberhauser AF, Schulten K, Fernandez JM, et al. Nature. 1999; 402:100–103. [PubMed: 10573426]
9. Li H, Linke WA, Oberhauser AF, Carrion-Vazquez M, Kerkvliet JG, Lu H, Marszalek PE, Fernandez JM. Reverse engineering of the giant muscle protein titin. Nature. 2002; 418:998–1002. [PubMed: 12198551]
10. Cao Y, Balamurali MM, Sharma D, Li H. A functional single-molecule binding assay via force spectroscopy. Proc Natl Acad Sci U S A. 2007; 104:15677–15681. [PubMed: 17895384]
11. Florin E-L, Rief M, Lehmann H, Ludwig M, Dornmair C, Moy VT, Gaub HE. Sensing specific molecular interactions with the atomic force microscope. Biosensors and Bioelectronics. 1995; 10:895–901.

12. Moy VT, Florin EL, Gaub HE. Intermolecular forces and energies between ligands and receptors. Science. 1994; 266:257–259. [PubMed: 7939660]
13. Fernandez JM, Li H. Force-clamp spectroscopy monitors the folding trajectory of a single protein. Science. 2004; 303:1674–1678. [PubMed: 15017000]
14. Marszalek PE, Lu H, Li H, Carrion-Vazquez M, Oberhauser AF, Schulten K, Fernandez JM. Mechanical unfolding intermediates in titin modules. Nature. 1999; 402:100–103. [PubMed: 10573426]
15. Fowler SB, Best RB, Toca Herrera JL, Rutherford TJ, Steward A, Paci E, Karplus M, Clarke J. Mechanical unfolding of a titin Ig domain: structure of unfolding intermediate revealed by combining AFM, molecular dynamics simulations, NMR and protein engineering. J Mol Biol. 2002; 322:841–849. [PubMed: 12270718]
16. Bosshart PD, Iordanov I, Garzon-Coral C, Demange P, Engel A, Milon A, Muller DJ. The transmembrane protein KpOmpA anchoring the outer membrane of Klebsiella. Structure. 2012; 20:121–127. [PubMed: 22244761]
17. Junker JP, Rief M. Single-molecule force spectroscopy distinguishes target binding modes of. Proc Natl Acad Sci U S A. 2009; 106:14361–14366. [PubMed: 19667195]
18. Dufrene YF, Hinterdorfer P. Recent progress in AFM molecular recognition studies. Pflugers Arch. 2008; 456:237–245. [PubMed: 18157727]
19. Prat A, Gomez-Sicilia A, Oberhauser AF, Cieplak M, Carrion-Vazquez M. Understanding biology by stretching proteins: recent progress. Curr Opin Struct Biol. 2010; 20:63–69. [PubMed: 20138503]
20. Oberhauser AF, Carrion-Vazquez M. Mechanical biochemistry of proteins one molecule at a time. J Biol Chem. 2008; 283:6617–6621. [PubMed: 18195002]
21. Fisher TE, Carrion-Vazquez M, Oberhauser AF, Li HB, Marszalek PE, Fernandez JM. Single molecule force spectroscopy of modular proteins in the nervous system. Neuron. 2000; 27:435–446. [PubMed: 11055427]
22. Bornschlogl T, Rief M. Single-molecule protein unfolding and refolding using atomic force microscopy. Methods Mol Biol. 2011; 783:233–250. [PubMed: 21909892]
23. Forman JR, Clarke J. Mechanical unfolding of proteins: insights into biology, structure and folding. Curr Opin Struct Biol. 2007; 17:58–66. [PubMed: 17251000]
24. Rounsevell R, Forman JR, Clarke J. Atomic force microscopy: mechanical unfolding of proteins. Methods. 2004; 34:100–111. [PubMed: 15283919]
25. Alegre-Cebollada J, Perez-Jimenez R, Kosuri P, Fernandez JM. Single-molecule force spectroscopy approach to enzyme catalysis. The Journal of biological chemistry. 2010; 285:18961–18966. [PubMed: 20382731]
26. Carrion-Vazquez M, Oberhauser AF, Fisher TE, Marszalek PE, Li H, Fernandez JM. Mechanical design of proteins studied by single-molecule force spectroscopy and protein engineering. Prog Biophys Mol Biol. 2000; 74:63–91. [PubMed: 11106807]
27. Puchner EM, Gaub HE. Force and function: probing proteins with AFM-based force spectroscopy. Curr Opin Struct Biol. 2009; 19:605–614. [PubMed: 19822417]
28. Helenius J, Heisenberg CP, Gaub HE, Muller DJ. Single-cell force spectroscopy. J Cell Sci. 2008; 121:1785–1791. [PubMed: 18492792]
29. Clausen-Schaumann H, Seitz M, Krautbauer R, Gaub HE. Force spectroscopy with single bio-molecules. Current opinion in chemical biology. 2000; 4:524–530. [PubMed: 11006539]
30. Engel A, Gaub HE, Muller DJ. Atomic force microscopy: a forceful way with single molecules. Curr Biol. 1999; 9:R133–136. [PubMed: 10074420]
31. Carrión-Vázquez, M.; Oberhauser, AF.; Díez, H.; Hervás, R.; Oroz, J.; Fernández, J.; Martínez-Martín, D. Protein Nanomechanics — as Studied by AFM Single-Molecule Force Spectroscopy Advanced Techniques in Biophysics. Arrondo, JLR.; Alonso, A., editors. Springer; Berlin Heidelberg: 2006. p. 163-245.
32. Zoldak G, Rief M. Force as a single molecule probe of multidimensional protein energy landscapes. Curr Opin Struct Biol. 2013; 23:48–57. [PubMed: 23279960]

33. Wiita AP, Perez-Jimenez R, Walther KA, Grater F, Berne BJ, Holmgren A, Sanchez-Ruiz JM, Fernandez JM. Probing the chemistry of thioredoxin catalysis with force. Nature. 2007; 450:124–127. [PubMed: 17972886]
34. Alegre-Cebollada J, Perez-Jimenez R, Kosuri P, Fernandez JM. Single-molecule force spectroscopy approach to enzyme catalysis. J Biol Chem. 2010; 285:18961–18966. [PubMed: 20382731]
35. Ma L, Xu MX, Oberhauser AF. Naturally Occurring Osmolytes Modulate the Nanomechanical Properties of Polycystic Kidney Disease Domains. J Biol Chem. 2010; 285:38438–38443. [PubMed: 20937836]
36. Kaiser CM, Bujalowski PJ, Ma L, Anderson J, Epstein HF, Oberhauser AF. Tracking UNC-45 chaperone-myosin interaction with a titin mechanical reporter. Biophys J. 2012; 102:2212–2219. [PubMed: 22824286]
37. Carrion-Vazquez M, Oberhauser AF, Fisher TE, Marszalek PE, Li H, Fernandez JM. Mechanical design of proteins studied by single-molecule force spectroscopy and protein engineering. Prog Biophys Mol Biol. 2000; 74:63–91. [PubMed: 11106807]
38. Berkovich R, Hermans RI, Popa I, Stirnemann G, Garcia-Manyes S, Berne BJ, Fernandez JM. Rate limit of protein elastic response is tether dependent. Proc Natl Acad Sci U S A. 2012; 109:14416–14421. [PubMed: 22895787]
39. Oberhauser AF, Marszalek PE, Erickson HP, Fernandez JM. The molecular elasticity of the extracellular matrix protein tenascin. Nature. 1998; 393:181–185. [PubMed: 9603523]
40. Law R, Carl P, Harper S, Dalhaimer P, Speicher DW, Discher DE. Cooperativity in forced unfolding of tandem spectrin repeats. Biophys J. 2003; 84:533–544. [PubMed: 12524305]
41. Steward A, Toca-Herrera JL, Clarke J. Versatile cloning system for construction of multimeric proteins for use in atomic force microscopy. Protein science: a publication of the Protein Society. 2002; 11:2179–2183. [PubMed: 12192073]
42. Fisher TE, Oberhauser AF, Carrion-Vazquez M, Marszalek PE, Fernandez JM. The study of protein mechanics with the atomic force microscope. Trends Biochem Sci. 1999; 24:379–384. [PubMed: 10500301]
43. Carrion-Vazquez M, Oberhauser AF, Fowler SB, Marszalek PE, Broedel SE, Clarke J, Fernandez JM. Mechanical and chemical unfolding of a single protein: a comparison. Proc Natl Acad Sci U S A. 1999; 96:3694–3699. [PubMed: 10097099]
44. Oroz J, Hervas R. Unequivocal single-molecule force spectroscopy of proteins by AFM using pFS vectors. Biophys J. 2012; 102:682–690. [PubMed: 22325292]
45. Garcia-Manyes S, Brujic J, Badilla CL, Fernandez JM. Force-clamp spectroscopy of single-protein monomers reveals the individual unfolding and folding pathways of I27 and ubiquitin. Biophys J. 2007; 93:2436–2446. [PubMed: 17545242]
46. Oberhauser AF, Hansma PK, Carrion-Vazquez M, Fernandez JM. Stepwise unfolding of titin under force-clamp atomic force microscopy. Proc Natl Acad Sci U S A. 2001; 98:468–472. [PubMed: 11149943]
47. Ainavarapu SR, Wiita AP, Huang HH, Fernandez JM. A single-molecule assay to directly identify solvent-accessible disulfide bonds and probe their effect on protein folding. J Am Chem Soc. 2008; 130:436–437. [PubMed: 18088123]
48. Oberhauser AF, Marszalek PE, Carrion-Vazquez M, Fernandez JM. Single protein misfolding events captured by atomic force microscopy. Nat Struct Biol. 1999; 6:1025–1028. [PubMed: 10542093]
49. Zhuang X, Rief M. Single-molecule folding. Curr Opin Struct Biol. 2003; 13:88–97. [PubMed: 12581665]
50. Perez-Jimenez R, Li J, Kosuri P, Sanchez-Romero I, Wiita AP, Rodriguez-Larrea D, Chueca A, Holmgren A, Miranda-Vizuete A, Becker K, Cho SH, Beckwith J, Gelhaye E, Jacquot JP, Gaucher EA, Sanchez-Ruiz JM, Berne BJ, Fernandez JM. Diversity of chemical mechanisms in thioredoxin catalysis revealed by single-molecule force spectroscopy. Nat Struct Mol Biol. 2009; 16:890–896. [PubMed: 19597482]

51. Szoszkiewicz R, Ainavarapu SR, Wiita AP, Perez-Jimenez R, Sanchez-Ruiz JM, Fernandez JM. Dwell time analysis of a single-molecule mechanochemical reaction. Langmuir. 2008; 24:1356–1364. [PubMed: 17999545]
52. Bhasin N, Carl P, Harper S, Feng G, Lu H, Speicher DW, Discher DE. Chemistry on a single protein, vascular cell adhesion molecule-1, during forced unfolding. J Biol Chem. 2004; 279:45865–45874. [PubMed: 15308645]
53. Perez-Jimenez R, Li J, Kosuri P, Sanchez-Romero I, Wiita AP, Rodriguez-Larrea D, Chueca A, Holmgren A, Miranda-Vizuete A, Becker K, Cho SH, Beckwith J, Gelhaye E, Jacquot JP, Gaucher EA, Sanchez-Ruiz JM, Berne BJ, Fernandez JM. Diversity of chemical mechanisms in thioredoxin catalysis revealed by single-molecule force spectroscopy. Nat Struct Mol Biol. 2009; 16:890–896. [PubMed: 19597482]
54. Perez-Jimenez R, Wiita AP, Rodriguez-Larrea D, Kosuri P, Gavira JA, Sanchez-Ruiz JM, Fernandez JM. Force-clamp spectroscopy detects residue co-evolution in enzyme catalysis. The Journal of biological chemistry. 2008; 283:27121–27129. [PubMed: 18687682]
55. Kosuri P, Alegre-Cebollada J, Feng J, Kaplan A, Ingles-Prieto A, Badilla CL, Stockwell BR, Sanchez-Ruiz JM, Holmgren A, Fernandez JM. Protein folding drives disulfide formation. Cell. 2012; 151:794–806. [PubMed: 23141538]
56. Lannon H, Vanden-Eijnden E, Brujic J. Force-clamp analysis techniques give highest rank to stretched exponential unfolding kinetics in ubiquitin. Biophys J. 2012; 103:2215–2222. [PubMed: 23200055]
57. Cao Y, Li H. Single-molecule force-clamp spectroscopy: dwell time analysis and practical considerations. Langmuir. 2011; 27:1440–1447. [PubMed: 21117668]
58. Grater F, Grubmuller H. Fluctuations of primary ubiquitin folding intermediates in a force clamp. J Struct Biol. 2007; 157:557–569. [PubMed: 17306561]
59. Brujic J, Hermans RI, Garcia-Manyes S, Walther KA, Fernandez JM. Dwell-time distribution analysis of polyprotein unfolding using force-clamp spectroscopy. Biophys J. 2007; 92:2896–2903. [PubMed: 17259284]
60. Schlierf M, Li H, Fernandez JM. The unfolding kinetics of ubiquitin captured with single-molecule force-clamp techniques. Proc Natl Acad Sci U S A. 2004; 101:7299–7304. [PubMed: 15123816]
61. Grandbois M, Beyer M, Rief M, Clausen-Schaumann H, Gaub HE. How strong is a covalent bond? Science. 1999; 283:1727–1730. [PubMed: 10073936]
62. Itoh H, Takahashi A, Adachi K, Noji H, Yasuda R, Yoshida M, Kinosita K. Mechanically driven ATP synthesis by F1-ATPase. Nature. 2004; 427:465–468. [PubMed: 14749837]
63. Fuson KL, Ma L, Sutton RB, Oberhauser AF. The c2 domains of human synaptotagmin 1 have distinct mechanical properties. Biophys J. 2009; 96:1083–1090. [PubMed: 19186144]
64. Rabbi M, Marszalek PE. Measuring protein mechanics by atomic force microscopy. CSH Protoc. 20072007 pdb prot4901.
65. Marszalek PE, Greenleaf WJ, Li H, Oberhauser AF, Fernandez JM. Atomic force microscopy captures quantized plastic deformation in gold nanowires. Proc Natl Acad Sci U S A. 2000; 97:6282–6286. [PubMed: 10841533]
66. Ma L, Xu M, Oberhauser AF. Single-molecule force spectroscopy of polycystic kidney disease proteins. Methods Mol Biol. 2012; 875:297–310. [PubMed: 22573448]
67. Bustamante C, Macosko JC, Wuite GJ. Grabbing the cat by the tail: manipulating molecules one by one. Nat Rev Mol Cell Biol. 2000; 1:130–136. [PubMed: 11253365]
68. Rabbi M, Marszalek PE. Measuring polysaccharide mechanics by atomic force microscopy. CSH Protoc. 20072007 pdb prot4900.
69. Burnham NA, Chen X, Hodges CS, Matei GA, Thoreson EJ, Roberts CJ, Davies MC, Tendler SJB. Comparison of calibration methods for atomic-force microscopy cantilevers. Nanotechnology. 2003; 14:1.
70. Hutter JL, Bechhoefer J. Calibration of atomic-force microscope tips. Rev. Sci. Instrum. 1993; 64:1868–1873.
71. Proksch R, Schäffer TE, Cleveland JP, Callahan RC, Viani MB. Finite optical spot size and position corrections in thermal spring constant calibration. Nanotechnology. 2004; 15:1344.

72. Cleveland JP, Manne S, Bocek D, Hansma PK. A nondestructive method for determining the spring constant of cantilevers for scanning force microscopy. Review of Scientific Instruments. 1993; 64:403–405.
73. Ma L, Xu M, Oberhauser AF. Single-molecule force spectroscopy of polycystic kidney disease proteins. Methods Mol Biol. 2012; 875:297–310. [PubMed: 22573448]
74. Bustamante C, Marko JF, Siggia ED, Smith S. Entropic elasticity of lambda-phage DNA. Science. 1994; 265:1599–1600. [PubMed: 8079175]
75. Stirnemann G, Giganti D, Fernandez JM, Berne BJ. Elasticity, structure, and relaxation of extended proteins under force. Proc Natl Acad Sci U S A. 2013
76. Vano E, Fernandez JM, Sanchez RM, Martinez D, Ibor LL, Gil A, Serna-Candel C. Patient radiation dose management in the follow-up of potential skin injuries in neuroradiology. AJNR Am J Neuroradiol. 2013; 34:277–282. [PubMed: 22859286]
77. Lasheras-Zubiate M, Navarro-Blasco I, Fernandez JM, Alvarez JI. Encapsulation, solid-phases identification and leaching of toxic metals in cement systems modified by natural biodegradable polymers. J Hazard Mater. 2012; 233:234–7.
78. Wang K, Forbes JG, Jin AJ. Single molecule measurements of titin elasticity. Prog Biophys Mol Biol. 2001; 77:1–44. [PubMed: 11473785]
79. Kellermayer MS, Smith SB, Granzier HL, Bustamante C. Folding-unfolding transitions in single titin molecules characterized with laser tweezers. Science. 1997; 276:1112–1116. [PubMed: 9148805]
80. Muller DJ, Baumeister W, Engel A. Controlled unzipping of a bacterial surface layer with atomic force microscopy. Proc Natl Acad Sci U S A. 1999; 96:13170–13174. [PubMed: 10557292]
81. Janshoff A, Neitzert M, Oberdorfer Y, Fuchs H. Force Spectroscopy of Molecular Systems-Single Molecule Spectroscopy of Polymers and Biomolecules. Angew Chem Int Ed Engl. 2000; 39:3212–3237. [PubMed: 11028062]
82. Oberhauser AF, Marszalek PE, Carrion-Vazquez M, Fernandez JM. Single protein misfolding events captured by atomic force microscopy. Nat Struct Biol. 1999; 6:1025–1028. [PubMed: 10542093]
83. Tskhovrebova L, Trinick J, Sleep JA, Simmons RM. Elasticity and unfolding of single molecules of the giant muscle protein titin. Nature. 1997; 387:308–312. [PubMed: 9153398]
84. Oberhauser AF, Hansma PK, Carrion-Vazquez M, Fernandez JM. Stepwise unfolding of titin under force-clamp atomic force microscopy. Proc Natl Acad Sci U S A. 2001; 98:468–472. [PubMed: 11149943]
85. Garcia-Manyes S, Dougan L, Badilla CL, Brujic J, Fernandez JM. Direct observation of an ensemble of stable collapsed states in the mechanical folding of ubiquitin. Proc Natl Acad Sci U S A. 2009; 106:10534–10539. [PubMed: 19541635]
86. Stahl SW, Puchner EM, Alexandrovich A, Gautel M, Gaub HE. A conditional gating mechanism assures the integrity of the molecular force-sensor titin kinase. Biophys J. 2011; 101:1978–1986. [PubMed: 22004752]
87. Puchner EM, Gaub HE. Exploring the conformation-regulated function of titin kinase by mechanical pump and probe experiments with single molecules. Angew Chem Int Ed Engl. 2010; 49:1147–1150. [PubMed: 20077447]
88. Puchner EM, Alexandrovich A, Kho AL, Hensen U, Schafer LV, Brandmeier B, Grater F, Grubmuller H, Gaub HE, Gautel M. Mechanoenzymatics of titin kinase. Proc Natl Acad Sci U S A. 2008; 105:13385–13390. [PubMed: 18765796]
89. Greene DN, Garcia T, Sutton RB, Gernert KM, Benian GM, Oberhauser AF. Single-molecule force spectroscopy reveals a stepwise unfolding of Caenorhabditis elegans giant protein kinase domains. Biophys J. 2008; 95:1360–1370. [PubMed: 18390597]
90. Puchner EM, Alexandrovich A, Kho AL, Hensen U, Schafer LV, Brandmeier B, Grater F, Grubmuller H, Gaub HE, Gautel M. Mechanoenzymatics of titin kinase. Proc Natl Acad Sci U S A. 2008; 105:13385–13390. [PubMed: 18765796]
91. Fernandez JM, Puerta F, Cousinou M, Dios-Palomares R, Campano F, Redondo L. Asymptomatic presence of Nosema spp. in Spanish commercial apiaries. J Invertebr Pathol. 2012; 111:106–110. [PubMed: 22820066]

92. Symens N, Mendez-Ardoy A, Diaz-Moscoso A, Sanchez-Fernandez E, Remaut K, Demeester J, Fernandez JM, De Smedt SC, Rejman J. Efficient Transfection of Hepatocytes Mediated by mRNA Complexed to Galactosylated Cyclodextrins. Bioconjug Chem. 2012

93. Perez-Jimenez R, Ingles-Prieto A, Zhao ZM, Sanchez-Romero I, Alegre-Cebollada J, Kosuri P, Garcia-Manyes S, Kappock TJ, Tanokura M, Holmgren A, Sanchez-Ruiz JM, Gaucher EA, Fernandez JM. Single-molecule paleoenzymology probes the chemistry of resurrected enzymes. Nat Struct Mol Biol. 2011; 18:592–596. [PubMed: 21460845]

94. Oberhauser AF, Carrion-Vazquez M. Mechanical biochemistry of proteins one molecule at a time. The Journal of biological chemistry. 2008; 283:6617–6621. [PubMed: 18195002]

95. Zhuang X, Rief M. Single-molecule folding. Curr Opin Struct Biol. 2003; 13:88–97. [PubMed: 12581665]

96. Oberhauser AF, Badilla-Fernandez C, Carrion-Vazquez M, Fernandez JM. The mechanical hierarchies of fibronectin observed with single-molecule AFM. J Mol Biol. 2002; 319:433–447. [PubMed: 12051919]

97. Schwaiger I, Kardinal A, Schleicher M, Noegel AA, Rief M. A mechanical unfolding intermediate in an actin-crosslinking protein. Nat Struct Mol Biol. 2004; 11:81–85. [PubMed: 14718927]

98. Junker JP, Ziegler F, Rief M. Ligand-dependent equilibrium fluctuations of single calmodulin molecules. Science. 2009; 323:633–637. [PubMed: 19179531]

99. Lee G, Abdi K, Jiang Y, Michaely P, Bennett V, Marszalek PE. Nanospring behaviour of ankyrin repeats. Nature. 2006; 440:246–249. [PubMed: 16415852]

100. Bullard B, Garcia T, Benes V, Leake MC, Linke WA, Oberhauser AF. The molecular elasticity of the insect flight muscle proteins projectin and. Proc Natl Acad Sci U S A. 2006; 103:4451–4456. [PubMed: 16537423]

101. Carrion-Vazquez M, Li H, Lu H, Marszalek PE, Oberhauser AF, Fernandez JM. The mechanical stability of ubiquitin is linkage dependent. Nat Struct Biol. 2003; 10:738–743. [PubMed: 12923571]

102. Dietz H, Rief M. Protein structure by mechanical triangulation. Proc Natl Acad Sci U S A. 2006; 103:1244–1247. [PubMed: 16432239]

103. Lu H, Isralewitz B, Krammer A, Vogel V, Schulten K. Unfolding of titin immunoglobulin domains by steered molecular dynamics simulation. Biophys J. 1998; 75:662–671. [PubMed: 9675168]

104. Sotomayor M, Schulten K. Single-molecule experiments in vitro and in silico. Science. 2007; 316:1144–1148. [PubMed: 17525328]

105. Gao M, Sotomayor M, Villa E, Lee EH, Schulten K. Molecular mechanisms of cellular mechanics. Phys Chem Chem Phys. 2006; 8:3692–3706. [PubMed: 16896432]

106. Lu H, Schulten K. Steered molecular dynamics simulations of force-induced protein domain unfolding. Proteins. 1999; 35:453–463. [PubMed: 10382673]

107. Krammer A, Lu H, Isralewitz B, Schulten K, Vogel V. Forced unfolding of the fibronectin type III module reveals a tensile molecular recognition switch. Proc Natl Acad Sci U S A. 1999; 96:1351–1356. [PubMed: 9990027]

108. Lee W, Zeng X, Zhou HX, Bennett V, Yang W, Marszalek PE. Full reconstruction of a vectorial protein folding pathway by atomic force microscopy and molecular dynamics simulations. The Journal of biological chemistry. 2010; 285:38167–38172. [PubMed: 20870713]

109. Mickler M, Dima RI, Dietz H, Hyeon C, Thirumalai D, Rief M. Revealing the bifurcation in the unfolding pathways of GFP by using single-molecule experiments and simulations. Proc Natl Acad Sci U S A. 2007; 104:20268–20273. [PubMed: 18079292]

110. Bryngelson JD, Onuchic JN, Socci ND, Wolynes PG. Funnels, pathways, and the energy landscape of protein folding: a synthesis. Proteins. 1995; 21:167–195. [PubMed: 7784423]

111. Dill KA, Chan HS. From Levinthal to pathways to funnels. Nat Struct Biol. 1997; 4:10–19. [PubMed: 8989315]

112. Burns JN, Orwig SD, Harris JL, Watkins JD, Vollrath D, Lieberman RL. Rescue of glaucoma-causing mutant myocilin thermal stability by chemical chaperones. ACS Chem Biol. 2010; 5:477–487. [PubMed: 20334347]

113. Ignatova Z, Gierasch LM. Inhibition of protein aggregation in vitro and in vivo by a natural osmoprotectant. Proc Natl Acad Sci U S A. 2006; 103:13357–13361. [PubMed: 16899544]
114. Tanaka M, Machida Y, Niu S, Ikeda T, Jana NR, Doi H, Kurosawa M, Nekooki M, Nukina N. Trehalose alleviates polyglutamine-mediated pathology in a mouse model of Huntington disease. Nat Med. 2004; 10:148–154. [PubMed: 14730359]
115. Liu R, Barkhordarian H, Emadi S, Park CB, Sierks MR. Trehalose differentially inhibits aggregation and neurotoxicity of beta-amyloid 40 and 42. Neurobiol Dis. 2005; 20:74–81. [PubMed: 16137568]
116. Woltjer RL, McMahan W, Milatovic D, Kjerulf JD, Shie FS, Rung LG, Montine KS, Montine TJ. Effects of chemical chaperones on oxidative stress and detergent-insoluble species formation following conditional expression of amyloid precursor protein carboxy-terminal fragment. Neurobiol Dis. 2007; 25:427–437. [PubMed: 17141508]
117. Uversky VN, Li J, Fink AL. Trimethylamine-N-oxide-induced folding of alpha-synuclein. FEBS Lett. 2001; 509:31–35. [PubMed: 11734201]
118. Sanchez R, Vano E, Ubeda C, Fernandez JM, Balter S, Hoornaert B. Influence of image metrics when assessing image quality from a test object in cardiac X-ray systems: Part II. J Digit Imaging. 2012; 25:537–541. [PubMed: 22223157]
119. Ainavarapu SR, Wiita AP, Huang HH, Fernandez JM. A single-molecule assay to directly identify solvent-accessible disulfide bonds and probe their effect on protein folding. J Am Chem Soc. 2008; 130:436–437. [PubMed: 18088123]
120. Dougan L, Fernandez JM. Tandem repeating modular proteins avoid aggregation in single molecule force spectroscopy experiments. J Phys Chem A. 2007; 111:12402–12408. [PubMed: 18020430]
121. Hartl FU. Chaperone-assisted protein folding: the path to discovery from a personal perspective. Nature medicine. 2011; 17:1206–1210.
122. Srikakulam R, Winkelmann DA. Myosin II folding is mediated by a molecular chaperonin. J Biol Chem. 1999; 274:27265–27273. [PubMed: 10480946]
123. Chow D, Srikakulam R, Chen Y, Winkelmann DA. Folding of the striated muscle myosin motor domain. J Biol Chem. 2002; 277:36799–36807. [PubMed: 12110670]
124. Srikakulam R, Winkelmann DA. Chaperone-mediated folding and assembly of myosin in striated muscle. J Cell Sci. 2004; 117:641–652. [PubMed: 14709723]
125. Barral JM, Hutagalung AH, Brinker A, Hartl FU, Epstein HF. Role of the myosin assembly protein UNC-45 as a molecular chaperone for myosin. Science. 2002; 295:669–671. [PubMed: 11809970]
126. Kachur TM, Pilgrim DB. Myosin assembly, maintenance and degradation in muscle: Role of the chaperone UNC-45 in myosin thick filament dynamics. Int J Mol Sci. 2008; 9:1863–1875. [PubMed: 19325835]
127. Kaiser CM, Bujalowski PJ, Ma L, Anderson J, Epstein HF, Oberhauser AF. Tracking UNC-45 chaperone-myosin interaction with a titin mechanical reporter. Biophys J. 2012; 102:2212–2219. [PubMed: 22824286]
128. Carrion-Vazquez M, Marszalek PE, Oberhauser AF, Fernandez JM. Atomic force microscopy captures length phenotypes in single proteins. Proc Natl Acad Sci U S A. 1999; 96:11288–11292. [PubMed: 10500169]

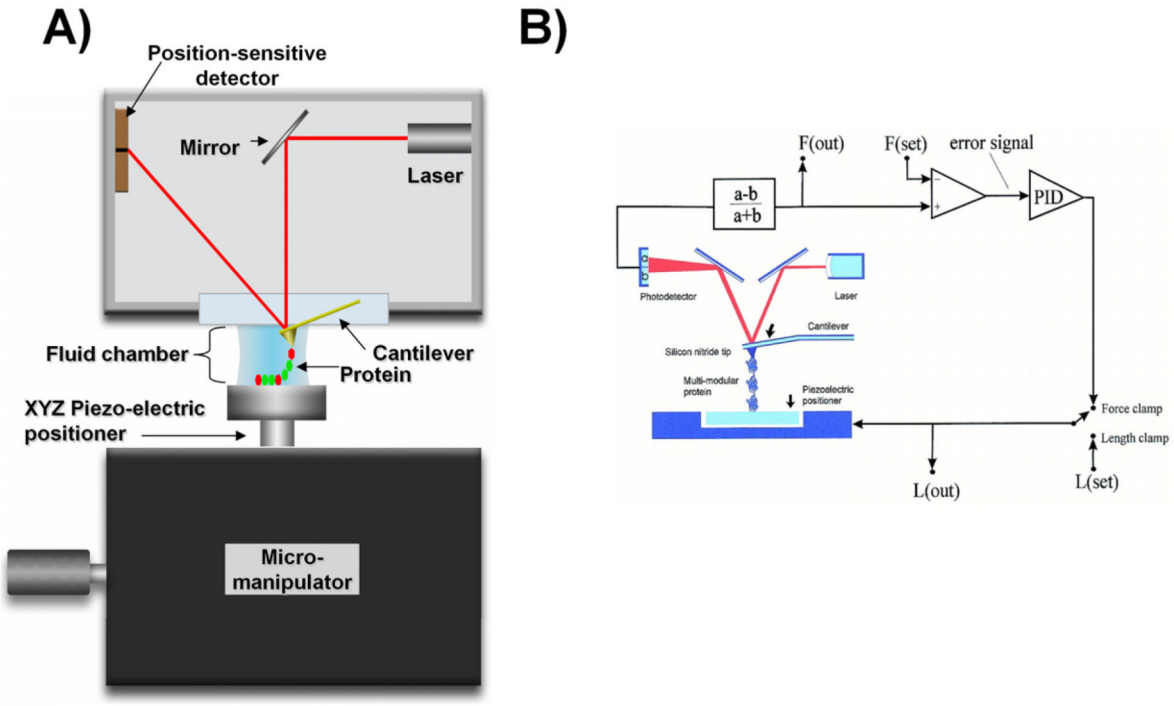

Figure 1. Schematic diagram of the AFM apparatus and associated control electronics

A) The AFM consists of two main parts: the scanner (Micromanipulator) and an optical head. The center point of the system is a small cantilever that functions as a microscopic spring. The cantilever is brought into contact with the sample and its bending is detected by shining a laser on its back; the light bounces off and is captured by a split photodetector (split into two regions: ‘a’ and ‘b ’photo-signals). A tiny deformation of a few nanometers causes a large alteration in the photovoltage of the detector due to optical amplification of the signal. The photovoltage is then converted into a force signal. The AFM is very sensitive it can measure forces in the range of pico-newtons and distances of only few angstroms. **B)** Two modes can be used to stretch single molecule: length-clamp or force-clamp modes. The standard length-clamp mode allows the control of the position (L) and measurement of the resulting force (F) which is calculated from the laser deflection (a − b)/(a + b). The force-clamp mode measures force and then compare it with a set value thus generating an error signal that is fed to a proportional, integral and differential amplifier (PID) whose output is connected directly to the piezoelectric positioner. Reproduced with permission from (84).

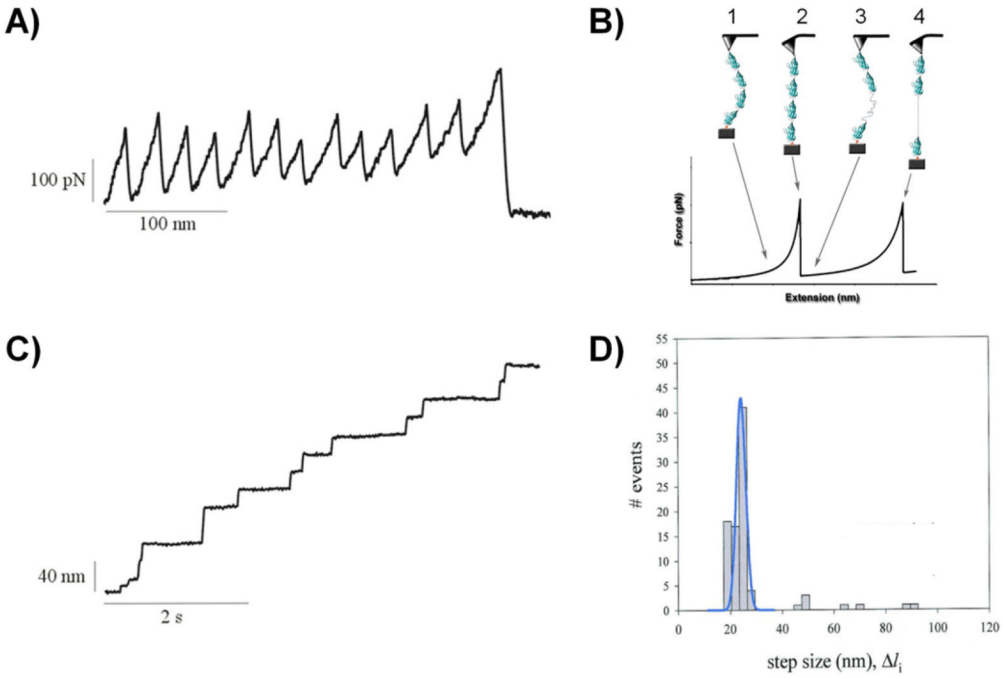

Figure 2. Protein unfolding events captured with length- and force-clamp AFM

A) Example of single protein unfolding events observed using AFM in length-clamp mode (A) and a force-clamp mode (C). **A)** In the length-clamp mode each force peak corresponds to the unfolding of individual domains. The recorded force-extension curve resembles a "sawtooth" pattern. Each force peak corresponds to the unfolding of a single protein domain. The spacing between force-peaks is related to the length of the polypeptide chain upon domain unfolding. In the case of the titin I27 domain the measured increase in contour length is about 28 nm which correspond to the unraveling of about 75 amino acids that were packed into core of the domain (128). The last peak shows the detachment of the protein from the cantilever. The unfolding peaks in the sawtooth pattern vary randomly in amplitude with an average value of ~200 pN which is a result of stochastic nature of the unfolding process of single domains. **B)** Cartoon diagram showing the different steps during the mechanical unfolding of a domain in a polyprotein. The AFM tip picks up a single protein (1) and starts pulling on it (2). When sufficient force is applied (around 200pN) the domains begin to unfold (3) until it's fully unfolded and reaches its maximum extension length (4). **C)** In the force-clamp mode the applied force is constant. The polyprotein unfolding resembles "staircase" pattern. Here each step of the extension-time curve corresponds to individual unfolding events and shows increases in the length of the protein. **D)** Frequency histogram of step sizes for the titin polyprotein (n = 99). The main peak is centered at 22.4 nm. Three minor peaks have average step size of about 48, 67, and 89 nm. The data were obtained at constant force of 147 pN. Reproduced with permission from (84).

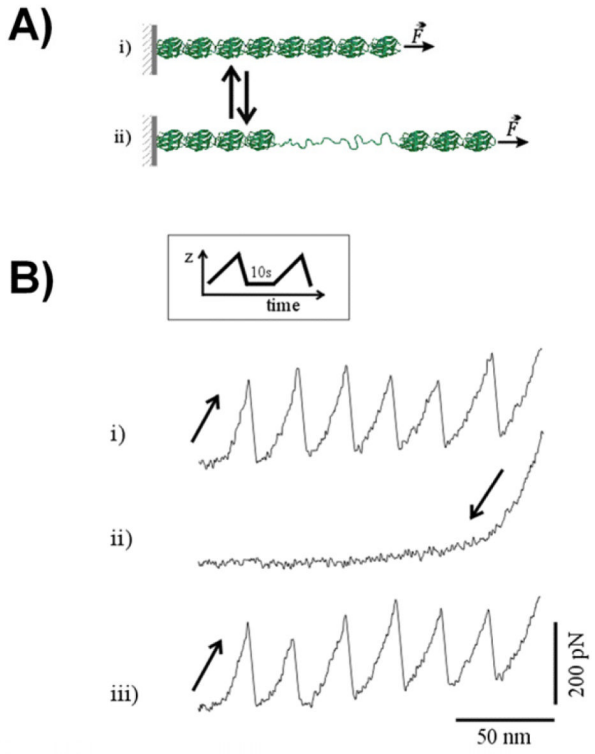

Figure 3. Capturing single protein refolding reactions using SMFS

A) Cartoon diagram showing the equilibrium between folded (i) and unfolded states (ii) of a polyprotein controlled by an applied mechanical force. **B)** Refolding kinetics probed with a double-pulse protocol (inset). The force/extension traces of an $I27_8$ polyprotein obtained by consecutively stretching (sawtooth pattern; trace i), relaxing (trace ii) and re-stretching after 10 s relaxation time (iii). All of the domains unfolded in the first pull and spontaneously refolded during the relaxed period. Single molecule experiments show the stochastic nature of the process which is exhibited by small difference between unfolding forces in following pulls. Reproduced with permission from (48).

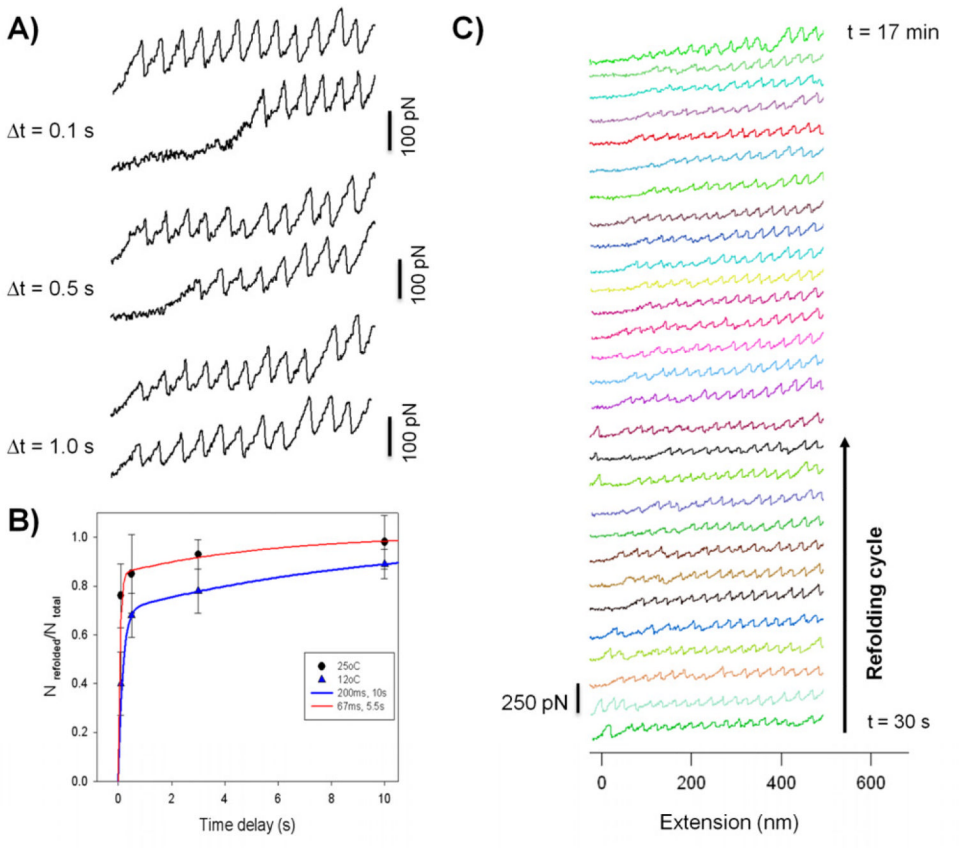

Figure 4. Unfolding and refolding kinetics of single titin-like proteins

A) Refolding of projectin domains depending on relaxation time (100ms, 1s, 10s). The refolding probability increases with increasing the time interval between stretching pulses. After 10s relaxation almost all domains refolded into their native state. **B)** Fraction of refolded domains as a function of the time delay between stretching pulses. The solid lines are a two-exponential fit of the data to the function $N_{refolded}/N_{total} = A_1 (1 - e^{-t\beta_1}) + A_2 (1 - e^{-\Delta t\beta_2})$. Considering the heterogeneous nature of the Ig-like domains, we attribute the biphasic folding kinetics to heterogeneity in folding kinetics among the different domains of projectin. **C)** A series of force-extension and relaxation cycles collected from a single projectin molecule. The delay time between each refolding cycle was about 20 seconds. In this example the protein was unfolded and refolded a total of 52 times. Reproduced with permission from (100).

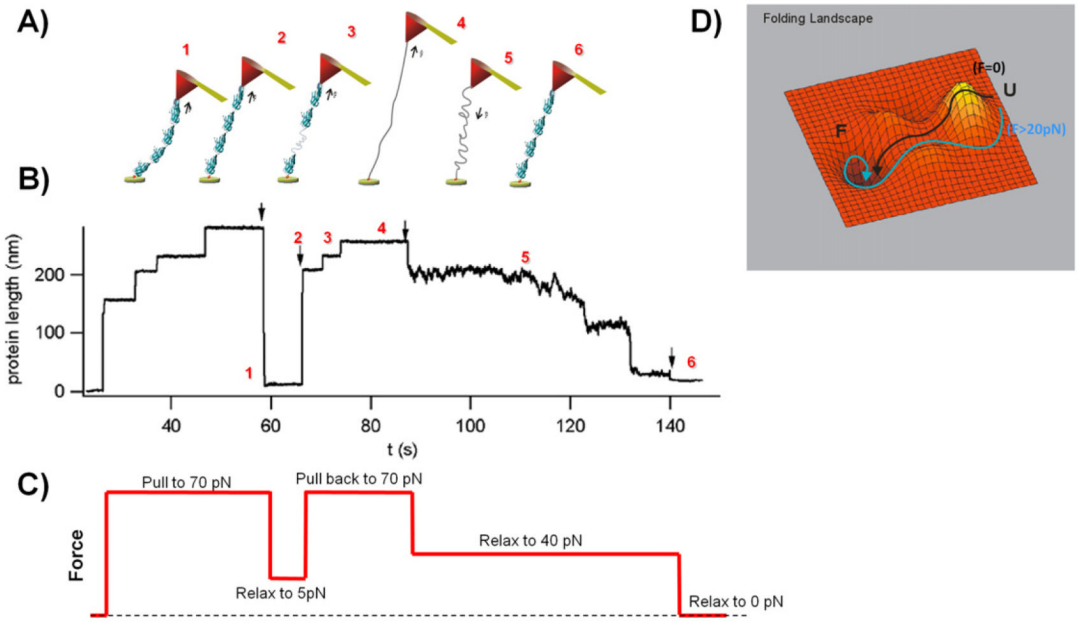

Figure 5. Collapse of unfolded protein domains under force

A) Cartoon representation of a projectin single molecule held under different force values. The cantilever is brought into a contact with a polyprotein (1), and then force is applied on the molecule (2). Protein domains start unfolding (3) until all of them are unfolded and protein reaches its maximum length (4). Then the force is released (5) until domains will refold to their native states. The cantilever was drawn at an angle for illustration purposes only. **B**) and **C)** In this experiment the protein was unfolded and extended at high force 70 pN. The observed steps correspond to the unfolding of several domains. Then the force was dropped to about 5 pN (marked by arrow); after 6 seconds the force was increased to 70 pN and, and after another 15 seconds it was lowered to 40 pN and finally to 0 pN. The applied force is shown in C). Reproduced with permission from (100). **D)** Schematic representation of the folding energy landscape under a stretching force (pathway in cyan) and no applied force (pathway in black). The diagram represents mapping of a possible conformations of a protein and their corresponding levels of Gibbs free energy. The protein's folded state corresponds to its free energy minimum.

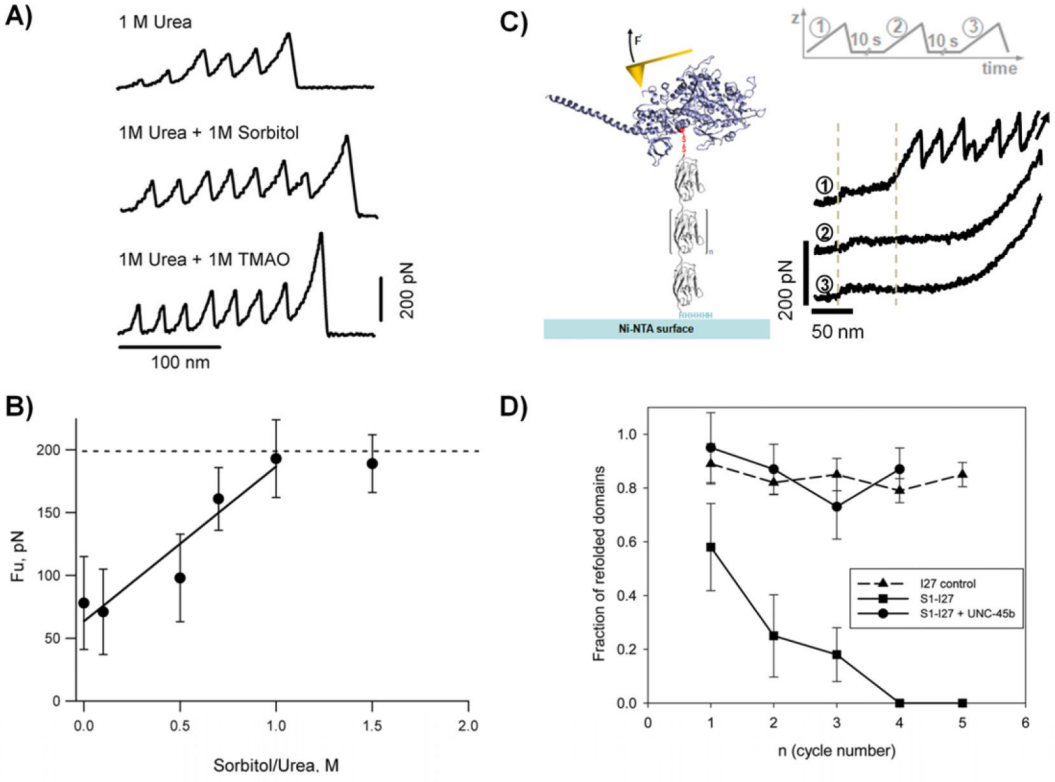

Figure 6. Probing the effects of osmolytes and molecular chaperones on protein folding and stability

A) Typical force-extension traces for a polyPKDd1-I27 protein obtained in different conditions: 1 M urea, 1 M urea + 1 M sorbitol, and 1 M urea + 1 M TMAO. **B)** Plot of the unfolding forces for PKD domains as a function of the sorbitol/urea ratio. The unfolding forces of PKDd1 steadily increases from 78 at 0 M, 71 at 0.1 M, 98 at 0.5 M, 161 at 0.7 M, to 193 at 1 M. The line represents a linear fit to the experimental data obtained below 1.0 sorbitol/urea ratio. **C)** Left) Diagram of a titin-derivatized myosin motor domain. Myosin (*blue*) was derivatized with a mechanical reporter (eight repeats of the titin I27 domain) carrying an N-terminal cysteine residue and a C-terminal His_6 tag. **C)** Right) Single derivatized myosins were subjected to repeated cycles of mechanical stretching, separated by a waiting time of 10 seconds at zero force. The characteristic I27 sawtooth pattern is seen in the initial unfolding trace (1). It is not present in the following traces (2 and 3), indicating that the unfolded myosin interferes with refolding of the I27 domains. The low-force plateau (around 30 pN) represents the unfolding of the myosin rod domain showing that it refolds independently from the motor domain. **D)** Plot of the refolding probability of titin I27 domains as a function of the stretching/relaxation cycles. Single S1-I27 proteins were subjected to repeated cycles of unfolding in the absence of chaperone (squares) or in the presence of 1 μM UNC-45 (circles). As a control the same experiment was performed using the I27 polyprotein (triangles). Reproduced with permission from (35, 36).